DEVELOPMENT OF FLUIDIC-BASED MEMRISTOR SENSOR FOR BIO-SENSING APPLICATION

by

NOR SHAHANIM BINTI MOHAMAD HADIS

Thesis submitted in fulfilment of the
requirements for the degree of
Doctor of Philosophy

April 2018

ACKNOWLEDGMENT

Alhamdulillah, all praises to Allah, unto Him belongs all knowledge and understanding.

In preparing this thesis, I was in contact with many peoples include researchers, academicians and practitioners. The have contributed towards my understanding and thoughts. I wish to express my sincere appreciation to my main supervisor Associate Prof. Dr. Asrulnizam Abd Manaf, for encouragement, guidance and critics. I am also very thankful to my co-supervisors Dr. Sukreen Hana Herman and Dr. Siti Hawa Ngalim for their guidance, advices and motivation. I am very honored and blessed to have had the opportunity to work with kind and supportive supervisors.

I also indebted to Ministry of Higher Education Malaysia for awarding me the scholarship that allowed me to conduct this study. I would also like to convey my gratitude to Universiti Sains Malaysia (USM) and Universiti Teknologi MARA (UiTM) for funding this research through various grants. I would like to convey my appreciation to the staff at Institute of Nano Optoelectronics Research and Technology (INOR) USM, especially to Mr Anas, Madam Bee Choo, Mr Yushamdan and Mr Jamil for their co-operation and technical assistance. Many thanks to my beloved colleagues Syira, Zaidi, Samihah and Belinda for their relentless helps, ideas and motivations.

Finally, I wish to express my love and gratitude to my husband, Suzasman, my father, Mohamad Hadis and my mother, Shakeynah for their support, understanding, patient encouragement throughout the tough journey of my PhD study. To my children, Hana, Syahmi, Hani and Asyraf, thanks for your understanding and patient, I love you very much. Without support from my family, I would not have been able to complete my study. Thank you very much.

TABLE OF CONTENTS

	Page
ACKNOWLEDGMENT	**ii**
TABLE OF CONTENTS	**iii**
LIST OF TABLES	**viii**
LIST OF FIGURES	**ix**
LIST OF ABBREVIATIONS	**xv**
LIST OF SYMBOLS	**xvii**
ABSTRAK	**xviii**
ABSTRACT	**xx**
CHAPTER ONE – INTRODUCTION	
1.1 Research Background	1
1.2 Problem Statements	3
1.3 Research Objectives	5
1.4 Scope of Research	5
1.5 Thesis Organization	7
CHAPTER TWO – LITERATURE REVIEW	
2.1 Introduction	9
2.2 Memristor History	9

2.3 Memristor Theory 14

2.4 Memristors in Bio-Sensing Applications 22

2.5 Memristive Materials and Electrode Materials for Memristor Devices 24

2.5.1 Memristive Materials 24

2.5.2 Electrode Materials 25

2.6 TiO_2 Thin Film Deposition Method 26

2.6.1 Physical Vapor Deposition 27

2.6.2 Chemical Vapor Deposition 28

2.6.3 Sol-Gel Deposition 28

2.7 TiO_2 Thin Film Patterning 29

2.7.1 Lift Off Technique 29

2.7.2 Sol-Gel Base Imprint Lithography Technique 33

2.7.3 Etching Technique 35

2.7.4 Site-Selective Deposition Technique 37

2.8 Memristor Characterization 40

2.9 Dengue Virus and Detection 42

2.10 Summary 48

CHAPTER THREE – METHODOLOGY

3.1 Introduction 50

3.2 Memristor Sensor Design Structure and Sensing Principles 50

3.2.1 Design Structure Evolution 53

3.2.2 First Structure: Simple Structure 56

3.2.3 Second Structure: Simple Structure with Wells 59

3.2.4 Third structure: Fluidic-Based Memristor Sensor Structure with Wells 61

3.2.5 Sensing Principles 63

3.2.5(a) First Structure 64

3.2.5(b) Second Structure 64

3.2.5(c) Third Structure 65

3.3 Memristor Sensor Fabrication 65

3.3.1 Substrate Preparation 68

3.3.2 TiO_2 Sol-Gel Preparation 68

3.3.3 Photoresist Mask Preparation for TiO_2 Patterning 69

3.3.4 TiO_2 Thin Film Deposition 70

3.3.4(a) Type A 70

3.3.4(b) Type B 71

3.3.5 Lift-Off Process 71

3.3.6 Aluminium Electrode Deposition 71

3.3.7 Surface Modification using Anti-Dengue Virus NS1 72

3.3.8 PDMS chamber preparation and attachment 74

3.4 Memristor Sensor Characterization and Analysis 77

3.4.1 I-V Characterization 79

3.4.2 Image Characterization 81

3.4.3 Off-On Resistance Ratio Analysis 82

3.4.4 Sensitivity 85

3.5 Summary 85

CHAPTER FOUR – RESULTS AND DISCUSSION

4.1 Introduction 87

4.2 First Structure: Simple Structure 88

4.2.1 Simple Structure: Type A 89

4.2.2 Simple Structure: Type B 93

4.2.3 Simple Structure: Sensing pH Liquid Based 97

4.2.4 Summary for First Structure Memristor Sensor 100

4.3 Second Structure: Simple Structure with Wells 101

4.3.1 Image characterization 102

4.3.2 I-V Characterization 105

4.3.3 Temperature Effect, Response Time and Accuracy 112

4.3.4 Comparison of the Type A and Type B Second Structure 118

4.3.5 Summary for Second Structure Memristor Sensor 120

4.4 Third structure: Fluidic Based Memristor Sensor with Wells 121

4.4.1 Image Characterization 122

4.4.2 I-V Characterization and Off-On Resistance Ratio Analysis 123

4.4.2(a) Off-on resistance ratio for 0.5 mm wells diameter 126

4.4.2(b) Off-on resistance ratio for 1.0 mm wells diameter 127

4.4.2(c) Off-on resistance ratio for 1.5 mm wells diameter 129

4.4.2(d) Off-on resistance ratio for 2.0 mm wells diameter 130

4.4.3 Summary of the Third Structure Memristor Sensor 136

4.5 Summary 136

CHAPTER FIVE – CONCLUSIONS AND FUTURE WORKS

5.1 Conclusions 138

5.2 Future Works 139

REFERENCES **141**

APPENDICES

Appendix A: Waiting Time Investigation for *I-V* Characterization

LIST OF TABLES

		Page
Table 2.1	Summary on suitable deposition method for four TiO_2 thin film patterning techniques	39
Table 2.2	Summary of operating characteristics and comparative costs of dengue diagnostic methods (WHO, 2009)	44
Table 2.3	Material, deposition method and patterning technique used in previous sensor/memristor/memristor sensor study	45
Table 3.1	TiO_2 thin film deposition summary	76
Table 4.1	Data of EDX mapping for four different post-bake temperature memristor	97
Table 4.2	List of liquids applied to simple structure Type A memristor sensor	98
Table 4.3	EDX measurement for Type A and Type B second structure memristor sensors	104
Table 4.4	Comparison between Type A and Type B second structure memristor sensor	119
Table 4.5	Top view of FESEM image of (a) free sensor, (b) sensor modified with dengue antibody and (c) modified-antibody sensor with dengue virus.	122
Table 4.6	Summary of third structure memristor sensor sensitivity for four wells diameters	132
Table 4.7	TiO_2 surface area for 416 nM dengue virus concentration according to wells diameter size	135
Table 4.8	Summary on memristor biosensors	137

LIST OF FIGURES

		Page
Figure 2.1	History of the memristor device	10
Figure 2.2	Structure of the memristor device by HP with a simplified equivalent circuit (Strukov et al., 2008)	12
Figure 2.3	Spice model of the memristor device by Biolek et al. (Biolek et al., 2009)	13
Figure 2.4	Schematic diagram of memristor device produce by Kamarozaman et al. in 2012	13
Figure 2.5	Proposed symbol of a memristor with φ-q curve (Chua, 1971)	16
Figure 2.6	Relationship of the four basic elements (Strukov et al., 2008)	16
Figure 2.7	Covalent bonding in Si semiconductor	17
Figure 2.8	Covalent bonding in TiO_2 semiconductor	17
Figure 2.9	(a) Ideal state memristor behavior (b) "off" state memristor (c) "on" state memristor (Miller, 2010)	19
Figure 2.10	Memristive conditions at different voltage potentials	21
Figure 2.11	Presentation of hysteresis loop analysis (I-V curve)	22
Figure 2.12	Silicon nanowire biosensor (Carrara et al., 2012)	23
Figure 2.13	Schematic diagram of fabricated noble metal/TiO_2 junctions (Hossein-Babaei et al., 2015)	26
Figure 2.14	Lift-Off Process for TiO_2 Patterning	30
Figure 2.15	Preparation of TiO_2 micropatterns (Li et al., 2013)	32
Figure 2.16	Thin film patterning process using sol-gel base nanoimprint lithography technique (Yoon et al., 2009)	34
Figure 2.17	Fabrication process of TiO_2 nano-wires (Francioso et al., 2008)	36
Figure 2.18	Conceptual process of site-selective elimination for the patterning of TiO_2 thin films from an aqueous solution (Masuda et al., 2003b).	38 38
Figure 2.19	Conceptual process for site-selective immersion to fabricate a patterned TiO_2 thin film from an aqueous solution (Masuda et al., 2002).	39

Figure 2.20	I-V curve of memristor biosensor in logarithmic scale focused on energy gap determination (Carrara et al., 2012)	41
Figure 2.21	Approximate time-line of primary and secondary dengue virus infections and the diagnostic methods that can be used to detect infection (WHO, 2009)	43
Figure 3.1	Methodology framework	52
Figure 3.2	Flowchart for the design process	54
Figure 3.3	Simple fluidic-based memristor sensor structure	58
Figure 3.4	Simple fluidic-based memristor sensor attached with PDMS chamber	59
Figure 3.5	Simple structure with wells memristor sensor	60
Figure 3.6	Simple structure with wells memristor sensor attached with PDMS chamber	61
Figure 3.7	Fluidic-based memristor sensor structure with wells	62
Figure 3.8	Fluidic-based memristor sensor structure with wells attached with PDMS chamber	63
Figure 3.9	General fabrication process for the three memristor structure	66
Figure 3.10	3-D presentation of common fabrication flow for second structure memristor sensor	67
Figure 3.11	Stirring process to produce sol-gel TiO_2	68
Figure 3.12	Film mask used for photoresist patterning (a) for simple structure, (b) for simple structure with wells and (c) for fluidic based memristor structure with wells	70
Figure 3.13	Method of Al electrode deposition using metal mask	72
Figure 3.14	The schematic for the three conditions of sensor characterization and analyses	73
Figure 3.15	Image of the plastic mould used to produce PDMS mould	74
Figure 3.16	Dimension of single unit plastic mould (PDMS chamber dimension) for one memristor sensor	75
Figure 3.17	Ready to use PDMS chamber	75
Figure 3.18	Grapical view of PDMS attachment process using adhesive bonding technique	76

Figure 3.19	Summary of the three memristor structures according to deposition, characterization and analysis	78
Figure 3.20	(a) Schematic diagram of the measurement setup for memristor sensor characterization; (b) the image of the workstation measurement platform	80
Figure 3.21	Memristor sensor measurement concept	80
Figure 3.22	Basic operation of the memristor device	81
Figure 3.23	(a) Measurement setup of FESEM and (b) Schematic of FESEM	82
Figure 3.24	I-V curve labelled with location “off” current and “on” current	83
Figure 3.25	Effect of different loop area towards the sensor sensing capability	84
Figure 4.1	Flowchart of result analysis for first structure memristor sensor	89
Figure 4.2	I-V curve of memristor devices for three different thickness of TiO_2 thin film (20, 30 and 50 nm)	90
Figure 4.3	Off-on resistance ratio of memristor devices for three different thicknesses of TiO_2 thin film (20, 30 and 50 nm)	91
Figure 4.4	Best fit line for off-on resistance ratio towards TiO_2 thin film thickness variations	92
Figure 4.5	I-V curve of memristor devices for four post-bake temperatures of 100 °C, 150 °C, 200 °C and 250 °C	93
Figure 4.6	Off-On resistance ratio of memristor devices for four post-bake temperatures of 100 °C, 150 °C, 200 °C and 250 °C	94
Figure 4.7	Best fit line for off-on resistance ratio towards post-bake temperature variations	94
Figure 4.8	Cross sectional view of memristor consisting of TiO_2 thin film and ITO layer	95
Figure 4.9	Low density EDX spectrum of simple structure memristor with post-bake temperature 100 °C	96
Figure 4.10	EDX mapping for memristor device at post-bake temperature of 100 °C (red dotted colour represented O and green dotted colour represented Ti)	96
Figure 4.11	I-V curve of memristor sensor in sensing different pH group liquids	98
Figure 4.12	Off-on resistance ratio of memristor sensor for different PH group liquids	99

Figure 4.13	Best fit line of off-on resistance ratio of memristor sensor for different pH value at 2 V reading voltage	99
Figure 4.14	Flowchart of result analysis for second structure memristor sensor	102
Figure 4.15	SEM image of Type A memristor sensor TiO_2 surface (a) 50,000 magnification, (b) 100,000 magnification, (c) 200,000 magnification and (d) 400,000 magnification.	103
Figure 4.16	SEM image of Type B memristor sensor TiO_2 surface (a) 50,000 magnification, (b) 100,000 magnification, (c) 200,000 magnification and (d) 400,000 magnification	104
Figure 4.17	Chemical structure of D-glucose liquid that contains multiple hydroxyl ion	105
Figure 4.18	I-V curve of Type A second structure memristor sensor	106
Figure 4.19	I-V curve of Type B second structure memristor sensor (Sol-gel spin coating)	107
Figure 4.20	I-V curve of Type B second structure memristor sensor (current (I) in logarithmic)	107
Figure 4.21	Off-on resistance ratio of Type A memristor sensor in sensing D-glucose concentrations	108
Figure 4.22	Off-on resistance ratio of Type B memristor sensor in sensing D-glucose concentrations	109
Figure 4.23	Off-on resistance ratio of Type A memristor sensor in sensing D-glucose concentrations at the reading voltage of 2.5 V	110
Figure 4.24	Off-on resistance ratio of Type B memristor sensor in sensing D-glucose concentrations at the reading voltage of 2.5 V	110
Figure 4.25	Off-on resistance ratio of Type A memristor sensor for different temperature environments	113
Figure 4.26	Average off-on resistance ratio of Type A memristor sensor (with error bar standard deviation) for the temperatures of 28 °C, 50 °C, 75 °C, 100 °C and 125 °C.	114
Figure 4.27	Response time analysis of Type A memristor sensor at the reading voltages of 1 V, 2 V and 3 V for 300 seconds.	115
Figure 4.28	Magnification of response time analysis for Type A memristor sensor at the reading voltages of 1 V, 2 V and 3 V for the first 10 seconds.	115

Figure 4.29	Off-on resistance ratio of Type A memristor sensor for accuracy measurement	116
Figure 4.30	Average off-on resistance ratio of Type A memristor sensor (with error bar standard deviation) for accuracy measurement	117
Figure 4.31	Logarithmic value of off-on resistance ratio of the sputtering and spin coating deposition method in detecting glucose liquid	118
Figure 4.32	Flowchart of result analysis process for third structure memristor sensor	121
Figure 4.33	A representative I-V curve for 2 mm-diameter wells	124
Figure 4.34	A representative of off-on resistance ratio of the memristor sensor	125
Figure 4.35	Off-on resistance ratio for third structure memristor sensor with wells diameter 0.5 mm applied with four concentrations dengue virus 1 NS1 (52, 104, 208 and 416 nM)	126
Figure 4.36	Off-on resistance ratio of third structure memristor sensor (wells diameter 0.5 mm) versus dengue virus concentration at the reading voltage of 0.25 V	127
Figure 4.37	Off-on resistance ratio for third structure memristor sensor with wells diameter 1.0 mm applied with four concentrations dengue virus 1 NS1 (51, 104, 208 and 416 nM)	128
Figure 4.38	Off-on resistance ratio of third structure memristor sensor (wells diameter 1.0 mm) versus dengue virus concentration at the reading voltage of 0.25 V	128
Figure 4.39	Off-on resistance ratio for third structure memristor sensor with wells diameter 1.5 mm applied with four concentrations dengue virus 1 NS1 (51, 104, 208 and 416 nM)	129
Figure 4.40	Off-on resistance ratio of third structure memristor sensor (wells diameter 1.5 mm) versus dengue virus concentration at the reading voltage of 0.25 V	130 130
Figure 4.41	Off-on resistance ratio for third structure memristor sensor with wells diameter 2.0 mm applied with four concentrations dengue virus 1 NS1 (51, 104, 208 and 416 nM)	131
Figure 4.42	Off-on resistance ratio of third structure memristor sensor (wells diameter 2.0 mm) versus dengue virus concentration at the reading voltage of 0.25 V	131
Figure 4.43	Off-on resistance ratio curve for four different wells diameter when applied with four concentrations dengue virus 1 NS1 (51, 104, 208 and 416 nM)	133

Figure 4.44 Off-on resistance ratio curve for four dengue protein concentrations applied to four wells diameters (0.5 mm, 1 mm, 1.5 mm, and 2 mm) 134

Figure 4.45 Sensing surface area for fluidic based memristor sensor 135

LIST OF ABBREVIATIONS

AC	Alternating Current
Ag	Silver
Al	Aluminium
Ar	Argon
Au	Gold
CVD	Chemical Vapor Deposition
DC	Direct Current
DENV	Dengue Virus
EDX	Energy Dispersive X-ray
FESEM	Field Emission Scanning Electron Microscope
GPTS	Glycidocypropyl-trimethoxysilane
HP	Hewlett Packard
ICP	Inductively Coupled Plasma
IgG	Immunoglobin G
IgM	Immunoglobin M
ITO	Indium Tin Oxide
I-V	Current-Voltage
LOR	Lift-Off Resist
NiSi	Nickel Silicide
NS1	Non-Structural 1
O	Oxygen
PBS	Phosphate-Buffered Saline
PDMS	Polydimethylsiloxane
PR	Photoresist

PSA	Prostate-Specific Antigen
Pt	Platinum
PVD	Physical Vapor Deposition
RF	Radio Frequency
RIE	Reactive Ion Etching
SAM	Self-Assembled Monolayers
SCS	Semiconductor Characterization System
SEM	Scanning Electron Microscope
Si	Silicon
SOI	Silicon on Insulator
Ta_2O_5	Tantalum Oxide
Ti	Titanium
TiO_2	Titanium Dioxide
UV	Ultraviolet
XHR	Extreme High Resolution
ZnO	Zinc Oxide

LIST OF SYMBOLS

μ_v	average ion mobility
C	capacitance
D	TiO_2 thin film thickness
d	wells diameter
I @ i	current
I_{OFF}	off current
I_{ON}	on current
φ	flux
λ	wavelength
M	memristance
Q @ q	charge
R	resistance
R_{OFF}	off resistance
R_{ON}	on resistance
S	sensitivity
V @ v	voltage
w	thickness of doped layer

PEMBANGUNAN PENDERIA MEMRISTOR BERASASKAN BENDALIR UNTUK APLIKASI BIO-PENDERIA

ABSTRAK

Diagnosis perubatan adalah bahagian penting dalam bidang perubatan. Pesakit biasanya perlu menunggu untuk suatu tempoh masa bagi mengesahkan sebarang jangkitan virus dengan melalui beberapa prosedur makmal piawai yang mengambil masa beberapa jam atau beberapa hari. Penghasilan penderia berasaskan bendalir dipercayai dapat menawarkan kaedah analisa jangkitan secara lebih cepat bagi tujuan pengesahan jangkitan virus dalam tempoh yang lebih singkat. Melihat daripada perspektif reka bentuk penderia, kawasan penderiaan tidak boleh dibiarkan terdedah kepada persekitaran kerana ia akan menyebabkan berlakunya penyejatan. Penghasilan penderia berasaskan bendalir mampu melindungi kawasan penderiaan dari persekitarannya dan dengan itu dapat mengelakkan penyejatan dan memberikan keputusan yang tepat. Kebanyakan penderia datang dalam struktur rumit, yang memerlukan proses fabrikasi yang kompleks. Penderia memristor yang dihasilkan dalam kajian ini mempunyai struktur yang ringkas dan dihasilkan menggunakan kaedah fabrikasi umum. Strukturnya yang mudah menjadikan penderia ini tidak mudah rosak dan mudah dikendalikan. Penderia memristor berasaskan bendalir yang dicadangkan dalam kajian ini menggunakan titanium dioksida sebagai bahan penderiaan, yang diapit di antara aluminium dan indium-tin-oksida sebagai elektrod atas dan bawah. Tiga struktur penderia telah direka bentuk dengan struktur ketiga menjadi struktur terakhir untuk penderiaan berasaskan bendalir. Struktur kedua dan ketiga mengandungi telaga untuk membolehkan cecair bertakung atau sebagai perangkap virus. Struktur pertama direka tanpa sebarang telaga dan digunakan bagi

mengesan beberapa cecair dari kumpulan pH yang berlainan. Hasil struktur pertama membantu pembangunan struktur kedua, dengan pembentukan telaga dan diuji dengan cecair yang mengandungi hidroksil ion. Hasil struktur kedua kemudian membantu pembangunan struktur ketiga yang direka untuk pelaksanaan penderiaan berasaskan bendalir yang digunakan untuk mengesan protein virus denggi NS1. Diameter telaga yang berbeza dari 0.5, 1.0, 1.5 dan 2.0 mm telah dihasilkan dan keupayaan pengesanan dikaji. Semua tiga struktur penderia memristor dicirikan dengan menggunakan kaedah pencirian arus-voltan dan pencirian imej. Daripada hasil pencirian arus-voltan, nisbah rintangan tutup-buka dikeluarkan, dan keupayaan penderiaan dikenalpasti. Struktur kedua diuji dengan empat kepekatan cecair D-glukosa, dan keputusan menunjukkan penderia yang dihasilkan menggunakan kaedah berputar sol-gel merekodkan kepekaan 120.65 $(mM)^{-1}$ berbanding dengan kaedah percikan yang hanya mencatatkan kepekaan 0.035 $(mM)^{-1}$. Bacaan kepekatan yang dicatatkan oleh kaedah berputar sol-gel menentukan kaedah pemendapan yang digunakan untuk menghasilkan penderia memristor struktur ketiga. Struktur ketiga kemudiannya diuji dengan empat kepekatan protein virus denggi NS1 dan penderia dengan diameter telaga 2.0 mm mencatatkan tingkah laku penderia memristor terbaik dengan kepekaan 0.0082 $(nM)^{-1}$, berbanding dengan diameter yang lebih kecil. Penderia memristor berasaskan bendalir dapat mengesan protein virus denggi NS1 dan sesuai untuk aplikasi bio-penderia.

DEVELOPMENT OF FLUIDIC-BASED MEMRISTOR SENSOR FOR BIO-SENSING APPLICATION

ABSTRACT

Medical diagnosis is a crucial part of the medical field. The patient is usually required to wait for a period of time to confirm any virus infection by going through some standard laboratory procedures that require several hours or days. It is believed that fluidic-based implementation can provide fast analytical judgement on the virus infection, with short confirmation period. Looking from a sensor design perspective, the sensing area of liquid sensor cannot be exposed to its surroundings because it will cause evaporation. The fluidic-based implementation covers the sensing area from its surroundings and thus can avoid evaporation and provides an accurate result. Most of the sensor comes in a complicated structure, which requires a complex fabrication process. The developed memristor sensor is simple in structure and is fabricated using general fabrication method. Its simple structure makes this sensor more robust and easy to handle. The fluidic-based memristor sensor proposed in this study used titanium dioxide as the sensing material which sandwiched between Aluminium and Indium-Tin-Oxide as top and bottom electrodes. Three sensor structures have been designed with the third structure become the final fluidic-based structure. The second and third structures contain wells to allow more liquid to stay or as virus entrapment. The first structure was designed without any wells and applied with different pH group liquids. The result of the first structure assisted the development of the second structure, with the formation of wells and applied with liquid containing hydroxyl ion. The result of the second structure then assisted the development of the third structure and applied for dengue virus NS1 glycoprotein detection. Different wells diameters of

0.5, 1.0, 1.5 and 2.0 mm were fabricated for the third structure and the detection capabilities were investigated. All the three structure memristor sensors were characterized using current-voltage and image characterization methods. From the current-voltage characterization result, the off-on resistance ratio is extracted, and the sensing capability is determined. The second structure applied with four D-glucose concentrations, and the results show that sol-gel spin coating method recorded the highest sensitivity of 120.65 $(mM)^{-1}$ compared to sputtering method with the recorded sensitivity is only 0.035 $(mM)^{-1}$. The sensitivity measurement recorded by the sol-gel spin coating method assists the decision for the deposition method for the third structure memristor sensor. The third structure was then applied with four dengue virus NS1 glycoprotein concentrations and the sensor with a well diameter of 2.0 mm recorded the strongest memristive behaviour with a sensitivity of 0.0082 $(nM)^{-1}$, compared with another smaller diameter. The fluidic-based memristor sensor is able to detect dengue virus NS1 protein and suitable for bio-sensing application.

CHAPTER ONE
INTRODUCTION

1.1 Research Background

In electronics history there are three basic passive elements commonly used which are resistors, inductors, and capacitors. In 1971, an engineer from the University of Berkeley, Leon O. Chua, predicted the existence of a new passive element, which is called a memristor. The word memristor comes from the words "memory resistor". The memristor is classified as another passive element with two terminals (the same as the resistor) which maintains a functional relationship between the time integrals of current and voltage. It is a memory resistor which functions as an information storage device. Chua predicted that the memristor would become the fourth passive element (Chua, 1971).

A physical model of the memristor was revealed by Hewlett-Packard (HP) in 2008 (Strukov et al., 2008). The model consists of a thin film semiconductor sandwiched between two plate metal electrodes (Strukov et al., 2008). The semiconductor material used by HP is titanium dioxide (TiO_2), and the metal electrode material used is platinum (Pt) (Williams, 2008). The TiO_2 is fabricated in two layers, one layer of perfect TiO_2 and one layer of TiO_2 with oxygen vacancies (Williams, 2008). Other semiconductor materials that show memristive behaviour are Si (Carrara et al., 2012, Puppo et al., 2014b) and ZnO (Chew and Li, 2013). Aluminium (Tedesco et al., 2012, Gale et al., 2012) and gold (Prodromakis et al., 2010) are also used as metal electrode materials due to their high conductivity.

Nowadays, many researchers are working on memristor designs for various applications. The fields that have been investigated include: memory (Ho et al., 2009, Zidan et al., 2013, Duan et al., 2014, Hu et al., 2012); photocatalytic (Sun et al., 2008);

neuromorphic systems (Jo et al., 2010); FPGAs (Chong and Xiao, 2011); computing (Joshua et al., 2012); and bio-sensing (Chen et al., 2010, Wang et al., 2010, Carrara et al., 2012, Sacchetto et al., 2011). Among those listed, memory application seems to have the largest potential compared with the others due to the device's ability to remember the past. This has been proven by just examining the large amount of research that has been produced in this field. Other than this, the bio-sensing application also offers a great future due to its stable sensing mechanism in memory application.

In 2012, memristor was invented as silicon nano-wire memristor bio-sensor by Carrara et al. applied in dry condition bio-detection (Carrara et al., 2012). Two years later, Puppo et al. developed a the same structure of silicon nano-wire memristor sensor for the dry condition bio-molecules detection (Carrara et al., 2012, Puppo et al., 2014b). For the two sensors, the sensing process takes more than one hour to do this process, which includes incubating, washing, and drying processes (Puppo et al., 2014b, Carrara et al., 2012). For the silicon nano-wire, the fabrication process involved to produce it is quite complicated which involved a lot of processes which will be discussed in Chapter Two.

In this thesis, a simple fluidic-based structure memristor sensor was developed to be applied for dengue virus Non-Structural 1 (NS1) protein detection. The dengue virus NS1 was chosen due to the early symptom detection inside human blood. NS1 can be detected as early on as day one of the infection, compared to Immunoglobulin M (IgM) and Immunoglobulin G (IgG) (WHO, 2009). IgM and IgG symptoms only can be detected in human blood as early on day four of the infection. This memristor sensor was applied in a fluidic-based platform which is suitable for human blood.

1.2 Problem Statements

Three main problems of dengue virus detection and current memristor sensor design have been figured out. The studies are based on current dengue virus sensors and current memristor biosensors.

No direct method can detect dengue virus NS1 in dengue virus infection confirmation

Medical diagnosis is a crucial part of the medical field. Medical practitioners must do some investigations in order to confirm whether patients are infected by a certain virus or not. Some parts of the process require a long waiting time for the patient to get the confirmed result. The dengue virus, when infected into humans, cannot be detected directly; the patient must go through a standard laboratory procedure that involves a few processes which requires one to two days to confirm the infection (WHO, 2009). The fastest dengue detection so far is 30 minutes IgM detection, inside human blood, using the rapid test IgM technique (WHO, 2009). Although the detection time is 30 minutes, IgM is a type of dengue symptom that can only be detected as early as the fourth day of infection. According to the World Health Organization (WHO), only dengue NS1 symptoms can be detected as early as the first day of infection (WHO, 2009). Due to this problem, the development of a memristor sensor to detect the dengue virus NS1 protein within 30 minutes is proposed in this thesis. This proposed memristor sensor can help medical practitioners to detect the dengue virus inside human blood as early as 30 minutes on the first day of infection through human blood.

Silicon nanowire memristor sensors are difficult to fabricate and have low robustness

The silicon nanowire memristor sensor, produced by previous researchers, has a complicated structure which is difficult to develop, and the nanometer size of the silicon nanowire makes it difficult to handle (Carrara et al., 2012, Puppo et al., 2014b). To obtain the silicon nanowire, the fabrication processes involve optical lithography with inductively coupled plasma (ICP) and isotropic ICP silicon etching, which are used to pattern the photoresist and to pattern the silicon nanowire, respectively. These two processes require a constant supply of carrier gas, which consequently increases the power consumption of the instrument. The rigid fabrication is due to the structure itself, which can easily break if applied with any force due to the small diameter of the nanowire, which is 600 nm. The sensor robustness is measured based on the handling capability whether easy to handle (high robustness) or difficult to handle (low robustness). Because of the small wire diameter, the sensor is difficult to handle, making it having a low robustness. Thus, the development of a new proposed memristor sensor structure, which is fabricated through a lift-off fabrication technique, provides a less complex fabrication process using common instruments such as ultraviolet exposure and deposition instruments. The proposed device also provides easy handling with a high robustness.

Current silicon nanowire memristor sensors are not integrated with a micro chamber which can cause sample evaporation

Bio-sensors usually sense liquid such as blood, urine, saliva, and others. When a liquid sample is placed or dispensed to the sensing surface there is a possibility that the liquid sample may evaporate (the process which the liquid turn to vapor when expose to air

for some period) (Oxford, 2012). The issue of media (liquid) evaporation was raised by Ettinger and Wittmann in their live-cell imaging studies (Ettinger and Wittmann, 2014). Ettinger and Wittman suggested the use of a sealed chamber to avoid media evaporation. Other researchers in the same field, Dailey et al., proposed the use of a sandwich of cover slips with the liquid sample in the middle, therefore making it difficult for the liquid to evaporate (Dailey et al., 2011). The evaporation will change the behaviour of the liquid and thus produce an inaccurate output. The implementation of a sensing principle in a fluidic-based platform is believed to be able to avoid the sample evaporation. This is because the sensing surface is fully covered by the micro chamber made by Polydimethylsiloxane (PDMS). The sample is not directly exposed to its surroundings and thus sample evaporation can be avoided.

1.3 Research Objectives

The objectives of this research are summarized as follows:

i. To design a simple structure fluidic-based bio sensor by implementing the memristor principle.
ii. To fabricate the memristor structure integrated with a micro chamber PDMS
iii. To investigate the memristive behaviour's effect on the fluidic-based memristor sensor in hydroxyl ion liquid detection.
iv. To characterize the memristive behaviour's effect on the fluidic-based memristor sensor in dengue virus NS1 protein detection.

1.4 Scope of Research

In this research, the focus has been to study the suitablility of memristors to be used as bio-sensors implemented in fluidic based platform. The work includes

memristor sensor design, memristor sensor fabrication, and memristor sensor characterization.

Three memristor structures have been fabricated, with the third structure becoming the final implemented fluidic-based memristor sensor structure for dengue NS1 detection. The material used as a sensing material is TiO_2 and the electrode material used is Aluminium (Al). The first structure is the basic structure which was designed for the purpose of studying the ability of the TiO_2 material in liquid sensing. The second structure was designed for the pupose of studying the effect of a wells toward the liquid detection, focussing on hydroxyl ion liquid detection. The third structure was designed for the purpose of implementing the sensor device as a real fluidic-based memristor sensor, and the behavior of the sensor towards the dengue virus NS1 protein was studied.

For the fabrication process, the TiO_2 thin film layer is deposited using two methods of radio frequency (RF) sputtering and sol-gel spin coating. For the RF sputtering method, the effect on different thicknesses was studied for the first structure. The best thickness was selected for the second structure fabrication. For the spin coating method, the effect on different post-bake temperatures was studied, and the best temperature was selected for the second structure fabrication. The lift-off technique was applied to get the patterned TiO_2. Patterning is very important in order to form a wells at the TiO_2 thin film layer. For the third structure, only the sol-gel spin coating method was used due to the high sensitivity recorded by the second structure of the spin coating method memristor. The third structure was then chemically modified with an anti-dengue virus NS1 glycoprotein monoclonal antibody before being presented with its ligand (NS1 glycoprotein).

The sensing capability of the memristor sensor was determined using two characterization methods of field emission scanning electron microscope (FESEM) and current-voltage (I-V) (using Keithly 4200 – semiconductor characterization system (SCS)). The FESEM was used to observe the surface morphology of the sensor and the SCS was used to obtained the graph of current versus voltage (I-V graph). Data from the *I-V* graph was then analyzed to get the off-on resistance ratio. The capability of the sensor is determined by the off-on resistance ratio. Different concentrations of the dengue virus NS1 protein were applied to the modified sensor in order to determine the sensitivity of the sensor. The sensitivity of the sensor is determined by the change of off-on resistance towards change in dengue virus concentrations.

1.5 Thesis Organization

This thesis is organized into five chapters. The content of each chapter is summarized as follows:

Chapter One explains, in a brief introduction, the study, which includes research background, problem statements, research objectives, scope of research, and significance of research.

Chapter Two provides an extensive review of memristor history, the memristive concept, and the use of memristors in bio-sensing applications. The common fabrication and characterization technique suitable for the memristor fabrication and characterization will also be reviewed in this chapter.

In Chapter Three, all the methods used in this research, including memristor sensor structure, memristor sensor fabrication, sensing principles, and memristor sensor characterization are described in detail.

The results obtained from the research works are analysed and discussed in Chapter Four. Three memristor sensor structures are analysed and discussed in various conditions, including a sensor without a liquid sample, a sensor with different pH samples, a sensor with different hydroxyl ion liquid concentrations, and a sensor with different dengue virus NS1 protein concentrations.

Finally, Chapter Five summarises the findings of this research. Recommendations for future work are also included in the chapter.

CHAPTER TWO
LITERATURE REVIEW

2.1 Introduction

This chapter discusses an overview of the memristor and includes its history and theory, followed by a review on memristor application in bio-sensing areas. An overview of the TiO_2 thin film fabrication method and patterning technique were also studied. A review of memristor characterization is also discussed. Finally, an overview of dengue virus and detection presented. All subtopics were addressed equally in order to come out with a new fluidic-based memristor sensor design for bio-sensing applications.

2.2 Memristor History

In electronics history, there are three basic passive elements commonly used, which are resistors, inductors, and capacitors. Inductors and capacitors have the ability to store energy for a certain period of time, which is determined by the time constant of the circuit, while resistors do not store energy. An overview of memristor history is summarized in Figure 2.1. The term “memristor” was introduced by an engineer from the University of Berkeley, Leon O. Chua, in 1971. Chua predicted the existence of a new element that he named a “memristor”, which is a contraction of the words “memory resistor” (Chua, 1971). Memristors are classified as another passive element with two terminals, the same as resistors, that maintain a functional relationship between the time integrals of current and voltage. It is a memory resistor which functions as an information storage device. Chua introduced the memristor as the fourth basic circuit element after resistors, inductors, and capacitors (Chua, 1971).

Chua was the first person to realize the existence of memristors, although there are some papers published before with the same behaviour as described by Chua, but from a different perception.

In 1962, Hickmott discovered that hysteretic current-voltage was observable in many nano-scale metal-oxide-metal devices with an oxide thickness of between 15nm to 1000nm (Hickmott, 1962). About a decade after that, Dearnaley published a paper presenting the electrical phenomenon in amorphous oxide film (Dearnaley et al., 1970). Dearnaley discovered that a thin layer of oxide films (10 nm – 2 μm) presented interesting electrical properties related to switching and memory phenomena. There are some other papers that have presented similar behaviours from different points of view (Waser and Aono, 2007, Scott and Bozano, 2007, Smits et al., 2005, Lai et al., 2006, Jeong et al., 2007, Jameson et al., 2007). Most of the papers address the memory application.

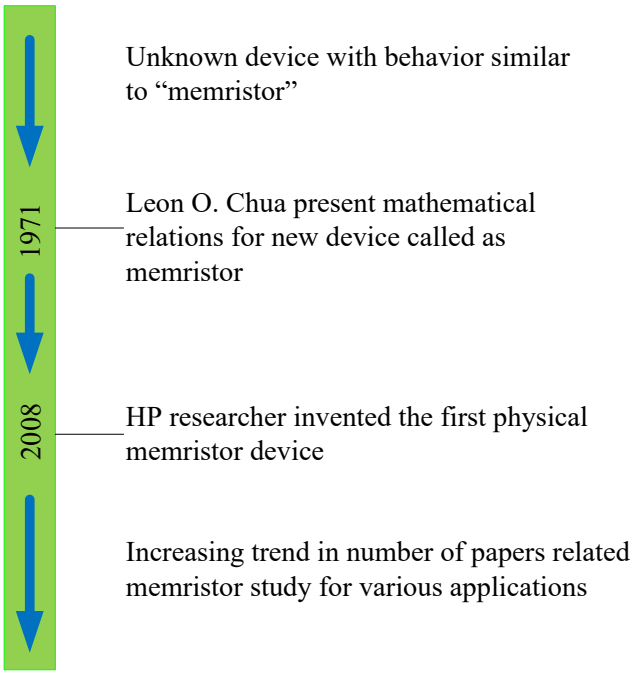

Figure 2.1: History of the memristor device

The first physical model of the memristor that relates to Chua's paper was revealed by Hewlett-Packard (HP) in 2008 (Strukov et al., 2008). Strukov et al. realized the relationship between nano-scale oxide thickness with Chua's prediction about memristors, and successfully fabricated a memristor device using the nano-scale oxide thickness concept. The model consists of a thin film semiconductor sandwiched between two plate metal electrodes (Strukov et al., 2008). Strukov et al. claim that memristive behaviour is naturally present in the nanoscale system due to solid-state electronic and ionic transport formation under external bias.

The semiconductor material used by HP is TiO_2 and the metal electrode material is platinum (Williams, 2008). The TiO_2 is fabricated in two layers; one layer of perfect TiO_2 and another layer of TiO_2 with oxygen vacancies, presented in Figure 2.2 (Strukov et al., 2008). The layer of perfect TiO_2 is labelled as "doped" and the layer of TiO_2 with oxygen vacancies is labelled as "undoped". The thickness of both layers is approximately 10 nm.

The undoped layer is represented by a resistor with a resistance value of "off" resistance (R_{OFF}), and the doped layer is represented by a resistor with a value of "on" resistance (R_{ON}). The simplified equivalent circuit for the memristor device is in a series connection between R_{ON} and $R_{OFF,}$ where the R_{ON} and R_{OFF} depends on the TiO_2 thin film thickness, D, and the thickness of doped layer, w.

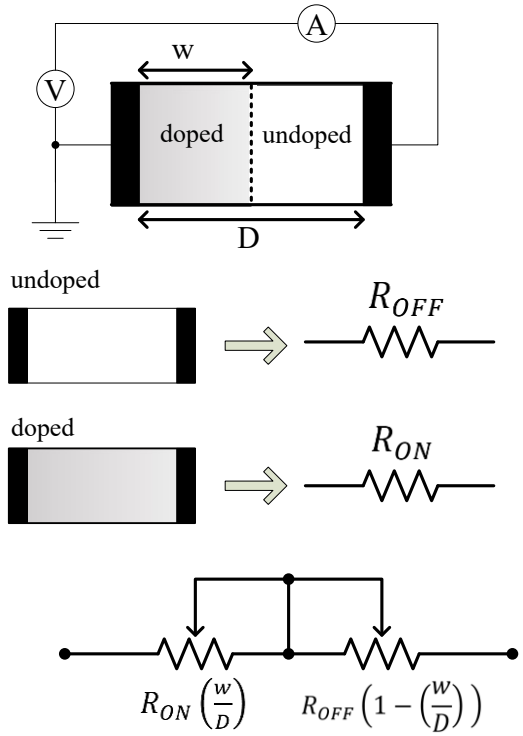

Figure 2.2: Structure of the memristor device by HP with a simplified equivalent circuit (Strukov et al., 2008)

Shortly after Strukov's paper was published, the researcher began to study and produce a suitable model for the memristor device produced in Strukov's paper. Published papers that present a memristor model design were written by Benderli et al., Biolek et al., Kavehei et al., and Miller et al. (Benderli and Wey, 2009, Biolek et al., 2009, Kavehei et al., 2010, Miller, 2010). The model which was produced by Biolek et al. is shown in Figure 2.3. The model was developed using spice, presented by a block-oriented diagram, with the memory effect performed by a feedback-controlled integrator.

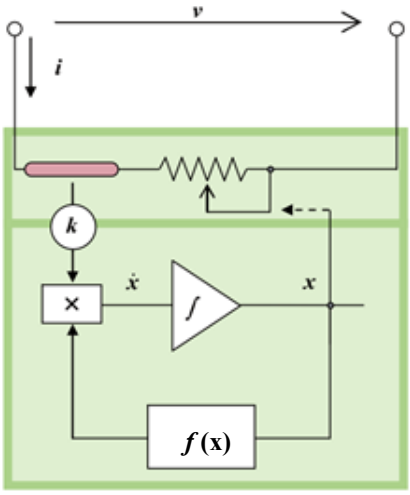

Figure 2.3: Spice model of the memristor device by Biolek et al.
(Biolek et al., 2009)

In 2012, Kamarozaman et al. published a top-bottom layout of memristor device which fabricated layer by layer (Kamarozaman et al., 2012). Bottom layer is indium tin oxide (ITO) and the top layer is platinum (Pt), both layers were used as negative and positive electrode respectively. Figure 2.4 shows the schematic diagram of the memristor device published by Kamarozaman et al. For the past few years, other researcher also implemented the same concept of top-bottom layout but the schematic layout of the device was not published to others (Gale et al., 2012, Strukov et al., 2008, Williams, 2008, Yakopcic et al., 2011).

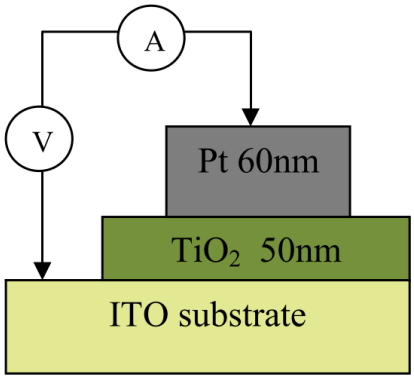

Figure 2.4: Schematic diagram of memristor device produce by
Kamarozaman et al. in 2012

Nowadays, many researchers are working on memristor design for various applications. The fields that have been investigated are: non-volatile memory (Ho et al., 2009, Ascoli et al., 2016, Duan et al., 2014, Ebong and Mazumder, 2011, Hu et al., 2012, Zidan et al., 2013), neuromorphic systems (Jo et al., 2010, Doolittle et al., 2009, Wang et al., 2017), FPGAs (Chong and Xiao, 2011), computing (Joshua et al., 2012, Wang et al., 2017), and sensing (Chen et al., 2010, Wang et al., 2010, Carrara et al., 2012, Sacchetto et al., 2011, Puppo et al., 2014b). All applications have a very high potential to be commercialized, with memory applications recorded in the highest number of published papers.

2.3 Memristor Theory

Memristors are unique and different compared to the other three basic circuit elements because of the memristor's ability to store memory of the past (Chua, 1971). In other words, if the memristor is turned off for a certain period of time and then turned on again, the memristor will still remember the amount of input applied before (Strukov et al., 2008). The capability is represented by the value of the present resistance of the memristor, which depends on the amount of electric charge which flowed through it in the past (Chua, 2011). This unique behaviour cannot be duplicated by any individual, or combination of, the three basic elements of resistors, inductors, and capacitors.

In the concept of circuit theory, resistors, inductors, and capacitors are defined by relationships between two circuit variables which are different from each other. There are four circuit variables in total to represent these relationships. The variables are current, voltage, charge, and flux-linkage. There are six possible combinations of two variables from the four variables. Five well-known relationships are described by

equations 2.1 – 2.5. Only one relationship remains undefined, the relationship between flux, φ and charge, q.

$$R = \frac{V}{I} \tag{2.1}$$

$$C = \frac{Q}{V} \tag{2.2}$$

$$L = \frac{\varphi}{I} \tag{2.3}$$

$$q(t) = \int_{-\infty}^{t} i(t)dt \; @ \; dq = idt \tag{2.4}$$

$$\varphi(t) = \int_{-\infty}^{t} v(t)dt \; @ \; d\varphi = vdt \tag{2.5}$$

Equations 2.1 – 2.3 present the basic axiomatic relationship for the three basic circuit elements of Resistor, R, Capacitor, C and Inductor, L. Equation 2.4 presents the relationship between charge and current and equation 2.5 presents the relationship between flux-linkage and voltage. The relationship between charge and flux-linkage is necessary in order to prove the relevance of the memristor proposed as the fourth basic element after resistor, inductor, and capacitor.

Chua's work has proposed the memristor's symbol and memristor's hypothetical φ-q curve, as shown in Figure 2.5. (Chua, 1971). The mathematical relationship is written by using equations 2.6 and 2.7. Equation 2.6 presents the electrical relationship, while equation 2.7 presents the magnetic relationship that relates between φ and q which was previously undefined.

$$v(t) = M\big(q(t)\big)i(t) \tag{2.6}$$

$$M(q) = \frac{d\varphi(q)}{dq} \tag{2.7}$$

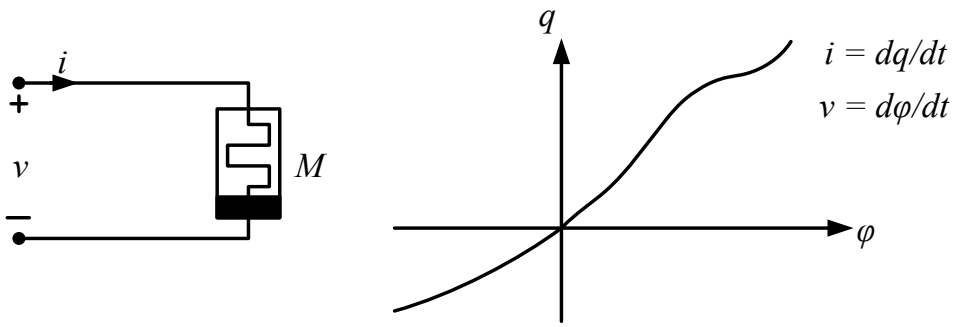

Figure 2.5: Proposed symbol of a memristor with φ-q curve
(Chua, 1971)

The relationship between the four circuit elements, resistor, inductor, capacitor, and memristor are shown in Figure 2.6, where equation 2.7 completes the relationship among the four variables (Strukov et al., 2008, Kavehei et al., 2010) . The memristance value, M depends on the change of flux in a function of charge over the change of charge.

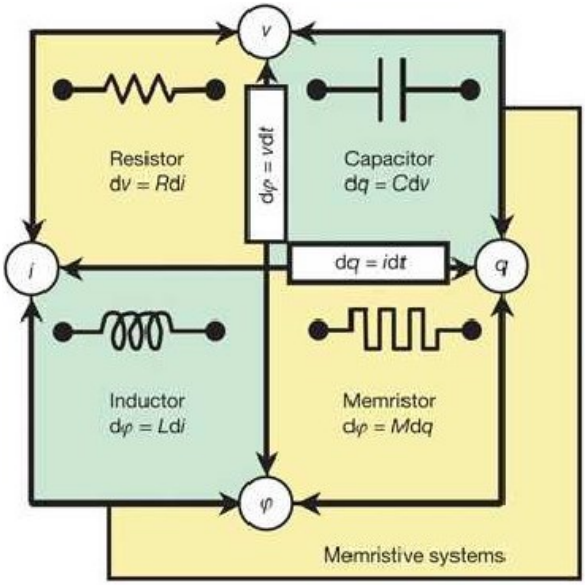

Figure 2.6: Relationship of the four basic elements
(Strukov et al., 2008)

The first material discovered to have memristive behaviour by Strukov et al. is TiO_2. TiO_2 has similar behaviour to silicon (Si) and titanium (Ti), coming from material group IV, and has 4 valence electrons. For Si, the valence electron is shared

among other Si to complete the valence shell to 8 electrons, as shown in Figure 2.7. While for Ti, the valence electron is shared with valence shell of oxygen atom (O) to complete the valence electrons as shown in Figure 2.8.

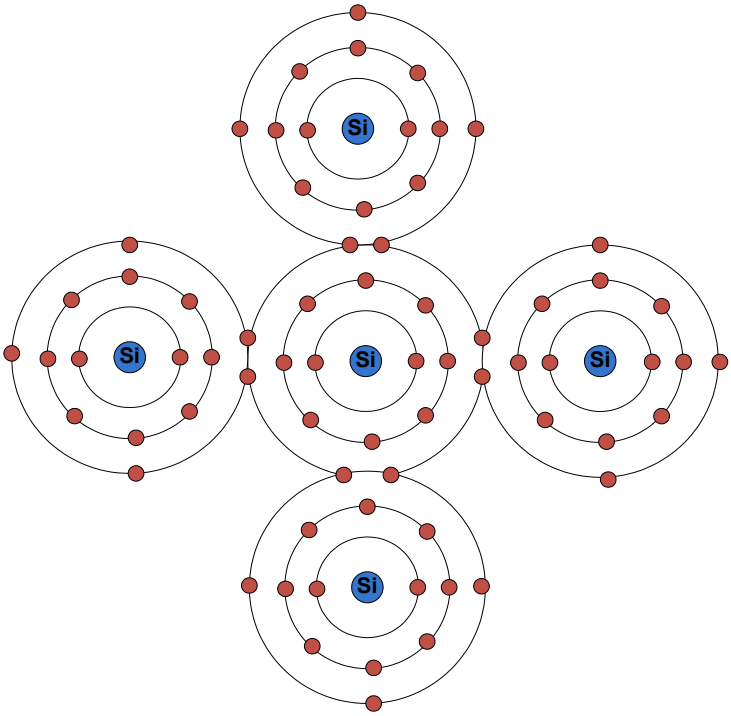

Figure 2.7: Covalent bonding in Si semiconductor

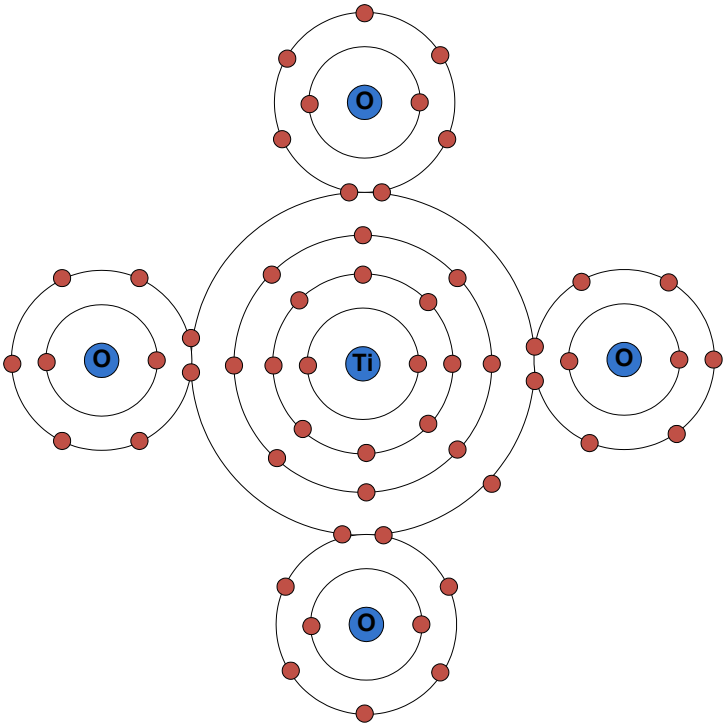

Figure 2.8: Covalent bonding in TiO_2 semiconductor

Semiconductor is generally pure state in highly resistive and it can de doped with another element to make it conductive. In TiO_2, the dopant that make it conductive is oxygen vacancies which tends to move at a high electric field (Anderson and Anderson, 2004). The dopant or oxygen vacancies moves in the same direction as the current direction, which makes the memristor work. However, the dopant mobility is not good for the transistor.

Putting a bias voltage across the thin film TiO_2 semiconductor, that has dopants only on one side, causes them to move into the pure TiO_2 on the other side, and thus lowers the resistance. Running the current in the other direction will then push the dopants back into place, increasing the TiO_2's resistance (Williams, 2008). A physical memristor that has been developed by Strukov et al. consists of a two-terminal device whose resistance depends on the magnitude, polarity, and length of time of the voltage applied to it. When the voltage is turned off, the resistance remains as it did just before it was turned off. This makes the memristor a non-linear, non-volatile memory device (Strukov et al., 2008).

The two-terminal memristor, introduced by Strukov et al. shown in Figure 2.2 uses TiO_2 as the resistive material and platinum as the electrode material. When a voltage is applied across the platinum electrodes, oxygen atoms in the material diffuse left or right, depending on the polarity of the voltage, which makes the material thinner or thicker, thus causing a change in resistance. It can be noted that transistors also use fixed-doped junctions, but unlike transistors, a memristor can change the doped region on the fly. The important thing about this is that, when the voltage is turned off, the oxygen atoms stay put, thus the resistance is "remembered." A memristor is not simply a digital on-or-off device. Since the doped region acts like a variable resistor, its state can be anywhere from 0 to 1, and this makes it a true analogue device. The diffusion

rate is 1 meter per second. That might sound slow, but it means that at nanometer scales, switching speeds can occur within nanoseconds (Williams, 2008).

Strukov et al. also developed the memristor model for the memristor device, and the relationship between voltage and current is represented in equation 2.8. This equation was developed for the simplest case of ohmic electronic conduction and linear ionic drift in a uniform field with average ion mobility, μ_v. (Strukov et al., 2008). Equation 2.11 was obtained by substituting 2.10 into 2.8 with the memristance value, M is in a function of charge, q.

$$v(t) = \left(R_{ON}\frac{w(t)}{D} + R_{OFF}\left(1 - \frac{w(t)}{D}\right)\right) i(t) \tag{2.8}$$

$$\frac{dw(t)}{dt} = \mu_V \frac{R_{ON}}{D} i(t) \tag{2.9}$$

$$w(t) = \mu_V \frac{R_{ON}}{D} q(t) \tag{2.10}$$

$$M(q) = R_{OFF}\left(1 - \frac{\mu_V R_{ON}}{D^2} q(t)\right) \tag{2.11}$$

In 2010, Miller presented three states of memristor in a structured view, as shown in Figure 2.9. The structure for an ideal memristor is shown in Figure 2.9(a), while Figure 2.9(b) and Figure 2.9(c) show the structure in "off" state and "on" state, respectively.

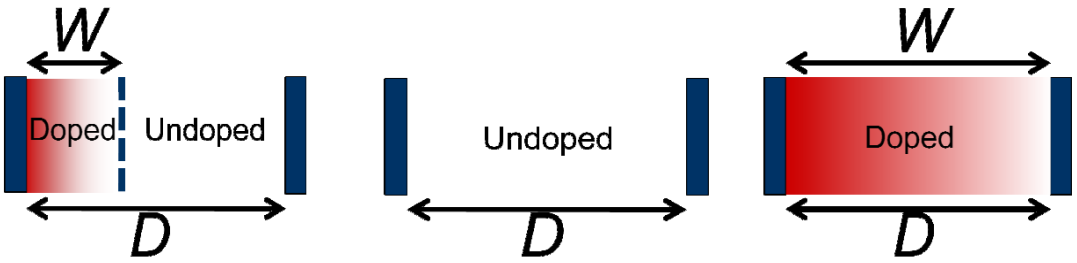

(a) (b) (c)

Figure 2.9: (a) Ideal state memristor behavior (b) "off" state memristor (c) "on" state memristor (Miller, 2010)

The thickness of the switching medium TiO_2 is constant, as described by depth, *D*. The thickness of the switching medium that is saturated by oxygen vacancies, which assist conduction, is described by the function *w*. If a positive voltage is applied to the doped side, the vacancies being positively charged will be repelled and drift into the undoped region, restricted by the mobility of the oxygen vacancies given by μ_v. Eventually, *w* will become equal to *D,* resulting in the "on" state, as shown in Figure 2.9(c). If the bias voltage is swapped, the oxygen vacancies will recede. Eventually *w* will be equal to 0, resulting in the "off" state, as the vacancies are completely pushed to one side, as shown in Figure 2.9(b). This behavior shows that the restriction on *w* is that it can never be greater than *D* or less than 0 (Miller, 2010).

In simulation, on resistance (R_{ON}) and off resistance (R_{OFF}) were set to any values. R_{ON} is low and R_{OFF} is very high. In practical application, the value of R_{ON} and R_{OFF} can be obtained from *I-V* characterization. Figure 2.10 shows the details of the memristive condition when various voltages are applied at a low frequency. The low frequency value is very low, almost zero, and therefore the direct current (DC) voltage is used to supply the memristor electrode instead of the alternating current (AC). The *I-V* characteristics of the memristor behave like hysteresis, but this is not a normal hysteresis. Memristor hysteresis is pinched at zero. This indicates the conductivity of memristor change when the applied voltage changes. It also indicates that the memristor stores the previous voltage, which is represented by its conductivity. This behaviour is only applicable if the frequency is low (where the time is long enough). If the frequency is high (where the sweep voltage is fast), the *I-V* curve will look like a normal resistor characteristic, which is linear.

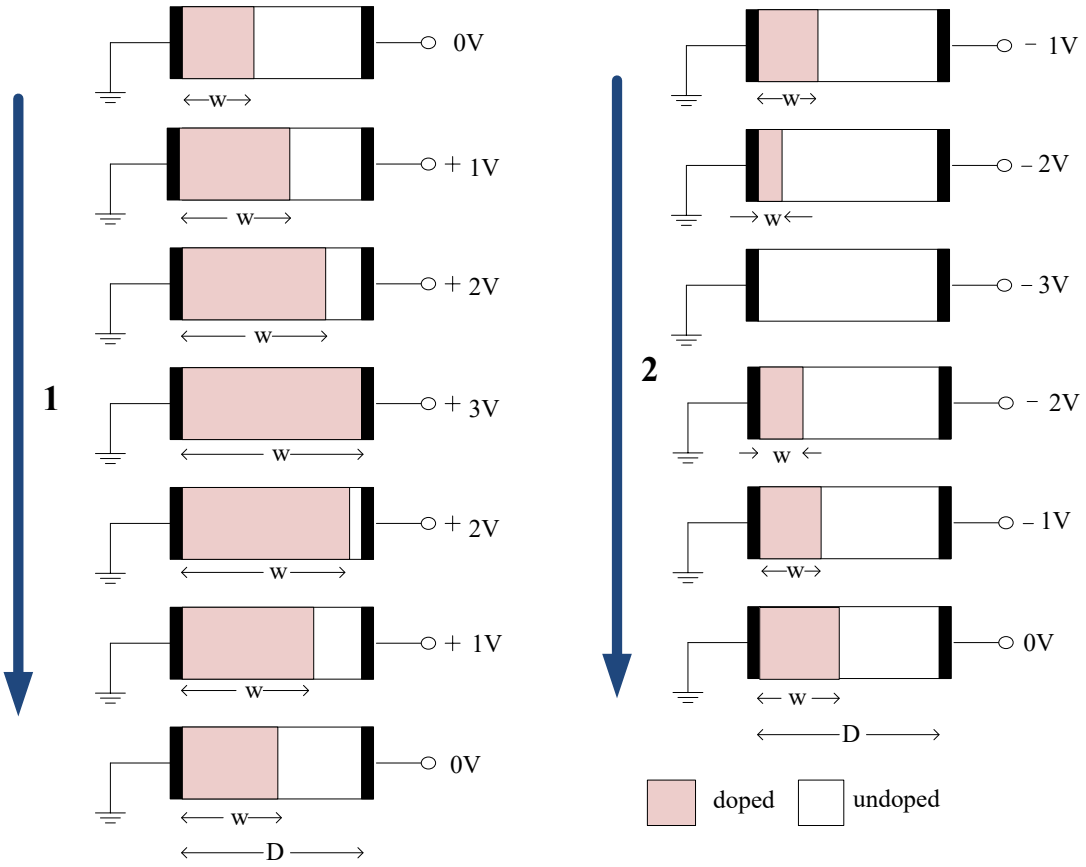

Figure 2.10: Memristive conditions at different voltage potentials

Figure 2.11 shows the graphical representation of the hysteresis loop analysis. At first, the voltage sweeps from 0 to +V (1-increase), then the voltage supply is decreased from +V to -V (2-decrease), and at last the voltage is increased from -V to 0 (3-increase) to complete the loop. The maximum and minimum voltage level depend on the thickness of the memristor, known as *D*.

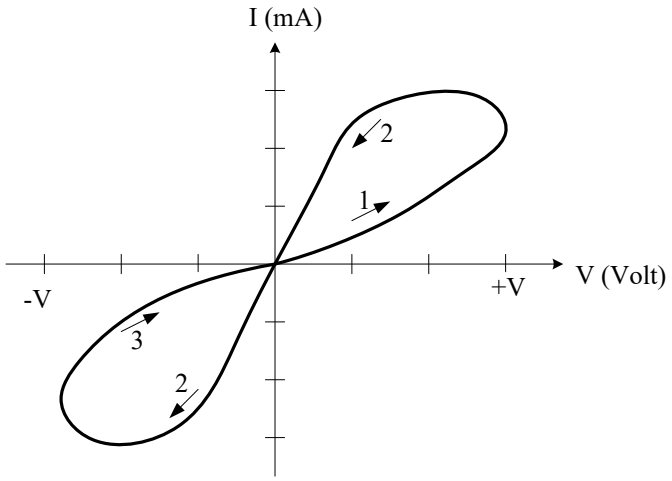

Figure 2.11: Presentation of hysteresis loop analysis (I-V curve)

2.4 Memristors in Bio-Sensing Applications

Research into bio-sensing applications started being investigated by Carrara et al. in 2012. Carrara et al. produced a silicon nanowire memristor sensor for bio-detection (Carrara et al., 2012, Sacchetto et al., 2011). The memristive material used for sensing is Silicon, while the electrode material used is Nickel Silicide. The silicon on insulator (SOI) used as substrate and the Si on the SOI were etched in order to produce a silicon nanowire. The image of the silicon nanowire is shown in Figure 2.12. Carrara et al. compare the energy gap of the silicon nanowire in two conditions: before antibody functionalization and after antibody functionalization. The sensor with the functionalized antibody records the increase in the energy gap compared with the sensor without antibody.

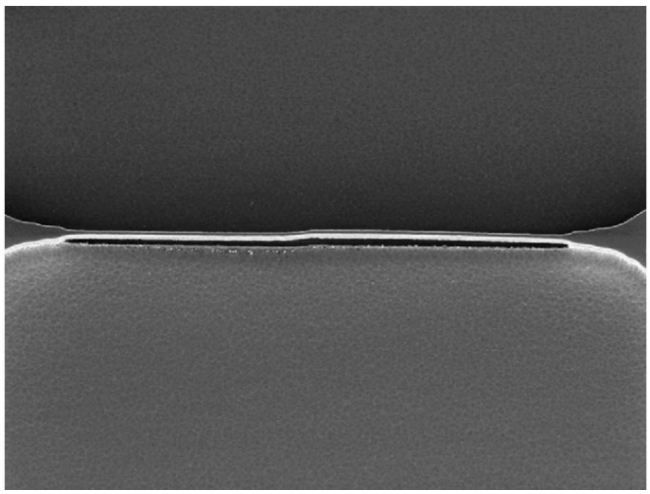

Figure 2.12: Silicon nanowire biosensor (Carrara et al., 2012)

The second publication related to bio-sensing was produced by Puppo et al. in 2014, and they also developed a silicon nanowire to sense bio-molecules (Puppo et al., 2014b). Puppo et al. used the same fabrication method as Carrara et al., and the biosensor behaviour was also observed through the energy gap. In 2015 and 2016, Tzouvadaki et al. published their work on silicon nanowire memristor sensors for a prostate-specific antigen (PSA) IgM detection (Tzouvadaki et al., 2015, Tzouvadaki et al., 2016). The latest publication was produced by Vallero et al. in 2016, which presents a microfluidic platform of devices for cancer prognosis (Vallero et al., 2016).

The behaviour of the developed memristor biosensors listed above was analysed by the difference in the voltage gap (Carrara et al., 2012, Puppo et al., 2014b, Tzouvadaki et al., 2016, Tzouvadaki et al., 2015, Vallero et al., 2016). Carrara, Puppo, Tzouvadaki, and Vallero used Nickel Silicide (NiSi) as the electrode material. In a recent paper published by Vallero et al., a comparison between two types of metal electrode, Aluminium (Al) and NiSi, were carried out (Vallero et al., 2016). The comparison shows that NiSi creates a change voltage gap for the memristor biosensor, from a zero-voltage gap to a nonzero voltage gap after surface functionalization. The

Al material did not provide a change in the voltage gap value for the condition before or after the surface functionalization process (Vallero et al., 2016).

The memristor sensors introduced by Carrara et al., Puppo et al., and Tzouvadaki et al. (2015) were tested in dry conditions. The sensing process takes more than one hour, which includes incubating, washing, and drying processes (Puppo et al., 2014b, Carrara et al., 2012). The latest research on memristor biosensor that was published in 2016 by Tzouvadaki et al. and Vallero et al. implemented a new sensing condition for the memristor device, which involves liquid detection with Tzouvadaki et al. implemented in microfluidic platform.

2.5 Memristive Materials and Electrode Materials for Memristor Devices

Two important things that need to be determined in order to produce a memristor device are determining the best memristive material (oxide material) and finding the best electrode material. A review of potential materials has been studied.

2.5.1 Memristive Materials

The first material presented by Strukov in 2008 for the first physical memristor is TiO_2. Besides TiO_2, many materials have been discovered to produce good memristive behaviour, including Zinc Oxide (ZnO) (Ayana et al., 2016, Chew and Li, 2013, Paul et al., 2014), Tantalum(V) Oxide (Ta_2O_5) (Torrezan et al., 2011) and Silicon (Si) (Carrara et al., 2012, Puppo et al., 2014a, Puppo et al., 2014b, Sacchetto et al., 2011, Tzouvadaki et al., 2015, Li et al., 2016). A study of the combination of various oxide thin-films in one memristor device was also performed by a few researchers. However, most of the papers used TiO_2 as their main material (Choi et al.,